

just assumed<sup>1</sup> such a behavior of the microcrystals within a grain to occur, even far away from cutoff. Very clearly his condition for the absence of secondary extinction in the most unfavorable case is no more restrictive than ours.

But there exists a physical difference between x-ray and neutron diffraction in the case of a ferromagnet which leads to the well-known transmission effects due to polarization. We have laid<sup>1</sup> great emphasis on the fact that marked extinction would show itself in a radical reduction of these transmission effects. Obviously if the cross section of the grain is no longer proportional to the cross section of the elementary scatterer, then a slight change of the latter, produced by magnetization, will not affect the total transmission very much. A study of the transmission effects therefore

permits insight into extinction effects even if sharp spectral resolution is not feasible.

In this connection an extinction problem deserves to be mentioned which is not treated in any exposition based on conventional x-ray theory. For wavelengths very near the cutoff it may occur that the angular width of the beam is larger than the deviation of the Bragg angle from  $\pi/2$ . This is contrary to the assumption underlying all x-ray theories; these x-ray treatments are realistic since one can see by a closer study that the case mentioned before can be established experimentally only with great difficulty. Still, it constitutes at least a mathematical problem which perhaps at some future time will find its experimental counterpart.

The author appreciates the cordial hospitality extended to him by the Brookhaven National Laboratory.

PHYSICAL REVIEW

VOLUME 88, NUMBER 5

DECEMBER 1, 1952

## Angular Correlations in the Reaction $F^{19}(p, \alpha\gamma)O^{16}$

J. SEED AND A. P. FRENCH

*Cavendish Laboratory, Cambridge, England*

(Received June 19, 1952)

The angular correlations between alpha-particles and gamma-rays in transitions between states of  $Ne^{20}$  and the low excited states of  $O^{16}$  have been studied at the 669-, 874-, and 935-kev resonances for proton capture in fluorine. The alpha-particle groups were separated magnetically from each other and from scattered protons. The results lead to definite assignments of spin and parity to the nuclear states involved, and show that the first four excited levels of  $O^{16}$  are consistent with a simple alpha-particle model for this nucleus. Where interference between states occurs in the reaction, the phase differences are in accord with the predictions of modern dispersion theory.

### I. INTRODUCTION

THE level structure of  $O^{16}$  has been the subject of many experimental and theoretical studies, and particular interest has been directed at those states which can be reached by the  $F^{19}(p, \alpha)$  reaction. (See, for example, the review article by Hornyak *et al.*<sup>1</sup>) The resonance levels in  $Ne^{20}$  formed in this reaction decay predominantly by alpha-particle emission; besides the transition to the ground state of  $O^{16}$ , four distinct alpha-particle groups have been observed, associated with transitions to the first four excited states of  $O^{16}$ . Much of the interest in these levels in  $O^{16}$  lies in the attempt to identify them with the low states of excitation of a bound system of four alpha-particles (Wheeler<sup>2</sup> and Dennison<sup>3</sup>). It is known that the first excited state of  $O^{16}$  (6.05 Mev) has spin zero and even parity [denoted by  $(0, +)$ ] (Devons and Lindsey<sup>4</sup>) and that the second excited state (6.13 Mev) has the designation  $(3, -)$  (Barnes *et al.*<sup>5</sup>). These do in fact correspond

(though in reversed order) to the first two excited states predicted by Wheeler and Dennison for a tetrahedral arrangement of alpha-particles, and the experiments described in this paper were carried out with the aim of extending the comparison to higher levels.

The levels in  $Ne^{20}$  formed by resonance capture of protons in fluorine seem to be of two kinds, namely, (a) those that can decay by emission of long-range alpha-particles to the ground state of  $O^{16}$ ; (b) those that emit short-range alpha-particles followed by gamma-rays. (From all levels of type (a) one also observes transitions to the well-known pair emitting state of  $O^{16}$  at 6.05 Mev.) It is usual to ascribe the absence of long-range alpha-particle emission for type (b) to a strict selection rule arising from the need to conserve total angular momentum ( $J$ ) and parity ( $P$ ) in the transitions; this is achieved by supposing that the  $Ne^{20}$  levels concerned have odd  $J$  with even  $P$ , or even  $J$  with odd  $P$ . A full discussion is given by Chao.<sup>6</sup> The present work was confined to levels of this type, and consisted of a study of angular correlations between the various alpha-particle groups and their associated gamma-rays.

<sup>1</sup> Hornyak, Lauritsen, Morrison, and Fowler, *Revs. Modern Phys.* **22**, 291 (1950).

<sup>2</sup> J. A. Wheeler, *Phys. Rev.* **52**, 1083 (1937).

<sup>3</sup> D. M. Dennison, *Phys. Rev.* **57**, 454 (1940).

<sup>4</sup> S. Devons and G. R. Lindsey, *Nature* **164**, 539 (1949).

<sup>5</sup> Barnes, French, and Devons, *Nature* **166**, 145 (1950).

<sup>6</sup> C. Y. Chao, *Phys. Rev.* **80**, 1035 (1950).

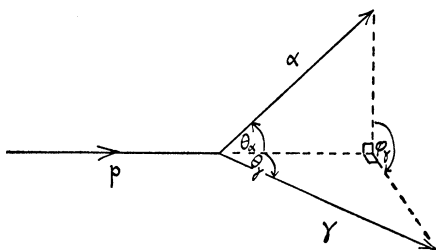
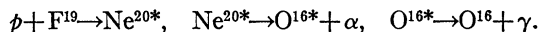


FIG. 1. The three-stage process.

## II. PLAN OF THE EXPERIMENTS

The reaction with which we are concerned is essentially a three-stage process, with two well-defined intermediate states:



It is thus possible to observe three types of angular correlation, which we can denote by  $(p, \alpha)$ ,  $(p, \gamma)$ , and  $(\alpha, \gamma)$ , respectively. In the usual experimental arrangement with a fluorine target and a collimated beam of protons the first two types correspond to straightforward angular distribution measurements. The third type must involve coincidence measurements in order to define a unique direction for the emitted alpha-particles. The three angular distribution functions are clearly related, since they are determined by the spins and parities of the nuclear states and by the orbital angular momenta of the captured and emitted particles, and it may be necessary to study all three types of correlation in order to obtain an unambiguous analysis of the process.

The proton capture resonances suitable for a complete study of this sort are those at 340-, 669-, 874-, and 935-keV proton energy, if we restrict attention to energies below 1 MeV (the highest energy available to us). These resonances are fairly narrow and have sufficiently large cross sections; the branching of the competing alpha-particle emissions to the gamma-emitting states of  $\text{O}^{16}$  (denoted in the usual way by  $\alpha_1$ ,  $\alpha_2$ , and  $\alpha_3$  in ascending order of excitation) changes markedly from one resonance to another. At the lowest resonance (340 keV) nearly all the transitions are to the  $\alpha_1$  level of  $\text{O}^{16}$  at 6.13 MeV. Studies at 340 keV of the  $(\alpha_1, \gamma)$  correlation (Arnold<sup>7</sup> and Barnes *et al.*<sup>5</sup>) and of the polarization of the gamma-rays (French and Newton<sup>8</sup>) have shown that the gamma-rays are electric octupole, and also that the compound state in  $\text{Ne}^{20}$  is  $(1, +)$  and is formed by  $s$  protons. The observed isotropy of both alpha-particles (Van Allen and Smith<sup>9</sup>) and gamma-rays (Devons and Hine<sup>10</sup>) with respect to the protons supports these conclusions.

We have used the definite assignment  $(3, -)$  for the

<sup>7</sup> W. R. Arnold, Phys. Rev. **79**, 170 (1950); **80**, 34 (1950).

<sup>8</sup> A. P. French and J. O. Newton, Phys. Rev. **85**, 1041 (1952).

<sup>9</sup> J. A. Van Allen and P. Smith, Phys. Rev. **59**, 501 (1941).

<sup>10</sup> S. Devons and M. G. N. Hine, Proc. Roy. Soc. (London) **A199**, 56 (1949).

6.1-MeV level in  $\text{O}^{16}$  to find spin values for the higher resonances in  $\text{Ne}^{20}$  by observing their  $(\alpha_1, \gamma)$  correlations. Measurements of the  $(\alpha_2, \gamma)$  and  $(\alpha_3, \gamma)$  correlations at these resonances have then enabled us to find the spins of the 6.9- and 7.1-MeV levels in  $\text{O}^{16}$ , with supporting evidence from the corresponding  $(p, \alpha)$  and  $(p, \gamma)$  angular distributions.

## III. THEORY OF THE METHOD

### (a) Statement of the Problems

Before describing the experiments we shall give a brief outline of the theory of a three-stage process as it applies to the present problem. Let the incident proton define a  $z$  axis, and let the compound state in  $\text{Ne}^{20}$  be denoted by  $C_r$ . Suppose that  $C_r$  breaks up with the emission of an alpha-particle at an angle  $\theta_\alpha$  to the proton beam, leaving an excited state of  $\text{O}^{16}$  denoted by  $C_s$ . Emission of a gamma-ray from  $C_s$  then takes place at an angle  $\theta_\gamma$  to the proton beam and in a plane at an angle  $\varphi_\gamma$  to the plane defined by the proton and alpha-particle directions. This is illustrated in Fig. 1. The differential cross section for emission of an alpha-particle into a solid angle  $d\Omega_\alpha$  at  $\theta_\alpha$  and a gamma-ray into  $d\Omega_\gamma$  at  $(\theta_\gamma, \varphi_\gamma)$  when the proton bombarding energy is  $E$  is then given by

$$d\sigma(E, \theta_\alpha, \theta_\gamma, \varphi_\gamma) = \pi\lambda^2 \left| \sum_{r,s} \frac{\langle A | H_1 | C_r \rangle \langle C_r | H_2 | C_s \rangle \langle C_s | H_3 | B \rangle}{E - E_r + \frac{1}{2}i\Gamma_r} \right|^2 d\Omega_\alpha d\Omega_\gamma,$$

where the numerator inside the modulus is a product of three matrix elements representing the formation and break-up of  $C_r$  and  $C_s$ . These matrix elements can then be resolved into an unknown factor depending on the specifically nuclear properties of the process and a transformation coefficient which describes the combination of angular momenta and is precisely known (Condon and Shortley<sup>11</sup>).

In the  $\text{F}^{19}(p, \alpha\gamma)$  reactions it is reasonable to assume that only one excited state of  $\text{Ne}^{20}$  and one excited state of  $\text{O}^{16}$  are involved for a given type of transition, but a summation must be made over (a) the spin states of the participating nuclei and (b) the various possible orbital momenta of the incoming protons and the outgoing alpha-particles. Since the final state in  $\text{O}^{16}$  has zero spin, only one type of multipole transition is possible for the gamma-radiation from a state of given spin and parity in the excited  $\text{O}^{16}$ . To take the analysis further it is convenient to discuss the three types of angular correlation separately.

### (b) $(p, \alpha)$ Correlations

In this case we are not concerned with the direction of emission of the gamma-ray, and the function de-

<sup>11</sup> E. U. Condon and G. H. Shortley, *The Theory of Atomic Spectra* (Cambridge University Press, Cambridge, 1935 and 1951).

scribing the angular distribution of alpha-particles relative to protons becomes

$$\begin{aligned} W(\theta_\alpha) &= \sum_{i, j_z} \sum_{J_{sz}} \left| \sum_l (2l+1)^{\frac{1}{2}} f_r(l) \langle j, j_z; l, 0 | J_r, J_{rz} \rangle \right. \\ &\quad \times \sum_{l'} f_s(l') \langle J_r, J_{rz} | J_s, J_{sz}; l', m' \rangle Y_{l', m'}(\theta_\alpha, 0) \left. \right|^2 \\ &= \sum_{i, j_z} \sum_{J_{sz}} \left| \sum_l (2l+1)^{\frac{1}{2}} f_r(l) \langle j, j_z; l, 0 | J_r, J_{rz} \rangle \right|^2 \\ &\quad \times \left| \sum_{l'} f_s(l') \langle J_r, J_{rz} | J_s, J_{sz}; l', m' \rangle Y_{l', m'}(\theta_\alpha, 0) \right|^2. \end{aligned}$$

Here  $j$  is the resultant spin (0 or 1) of the  $F^{19}$  nucleus and a proton, and  $J_r, J_s$  are the total angular momenta of the excited  $Ne^{20}$  and  $O^{16}$ , respectively.  $f_r(l)$  and  $f_s(l')$  are complex factors describing the probability amplitudes associated with the different orbital momenta.  $Y_{l', m'}$  is a spherical harmonic. (It should be noted that the  $Ne^{20}$  levels with which we are concerned can arise only from the spin state  $j=1$ .)

In the present reaction it is sufficient to consider the two lowest possible values of  $l$  and  $l'$ . (For the latter only one value is in fact allowed for some transitions by the conservation rules for total angular momentum and parity.)

### (c) $(p, \gamma)$ Correlations

In this case we must integrate the differential cross section over all directions of the outgoing alpha-particle. Since the alpha-particle wave is described by a superposition of spherical harmonics, which are orthogonal, the integration eliminates interference between the different  $l'$ , and the angular distribution of gamma-rays becomes

$$\begin{aligned} W(\theta_\gamma) &= \sum_{i, j_z} \sum_{l', m'} \left| \sum_l (2l+1)^{\frac{1}{2}} f_r(l) \langle j, j_z; l, 0 | J_r, J_{rz} \rangle \right. \\ &\quad \times f_s(l') \langle J_r, J_{rz} | J_s, J_{sz}; l', m' \rangle \mathbf{E}_{J_s^{J_{sz}}}(\theta_\gamma, \varphi_\gamma) \left. \right|^2 \\ &= \sum_{i, j_z} \sum_{l', m'} \left| \sum_l (2l+1)^{\frac{1}{2}} f_r(l) \langle j, j_z; l, 0 | J_r, J_{rz} \rangle \right|^2 \\ &\quad \times \left| f_s(l') \langle J_r, J_{rz} | J_s, J_{sz}; l', m' \rangle \right|^2 \\ &\quad \times \left| \mathbf{E}_{J_s^{J_{sz}}}(\theta_\gamma, \varphi_\gamma) \right|^2. \end{aligned}$$

$\mathbf{E}_{J_s^{J_{sz}}}$  is the matrix element for the radiative transition to the ground state of  $O^{16}$ . All other quantities have the same meaning as before.

### (d) $(\alpha, \gamma)$ Correlations

Since we are now interested in the angular distribution of the gamma-rays relative to the alpha-particles, it is convenient to use the alpha-particle direction to define a new axis of  $z$ . Let us call it  $z'$ . The problem can then be stated as follows: We quantize the system  $C_r$  along an axis which is the direction of an incident proton. We then wish to quantize it again along the direction  $z'$  before going through those transformations

that correspond to the break-up processes. A compound state characterized by given values of  $J$  and  $J_z$  with respect to the original  $z$  axis is then described as a *coherent* superposition of states of the same  $J$  but with all possible values of  $J_{z'}$  between  $+J$  and  $-J$ , and the probability amplitude associated with a given  $J_{z'}$  is given by a transformation coefficient  $C_{J_z, J_{z'}}$ . In our experiments  $z'$  is at right angles to  $z$ , so that  $C_{J_z, J_{z'}}$  can be written as the amplitude associated with  $J_x$  in a scheme in which  $J_z$  is diagonal. Once one has set up the matrix of  $J_x$  (e.g., Schiff<sup>12</sup>) the  $C$ 's can be very easily found; they are solutions to equations of the type

$$\langle J_x | J_x - 1 \rangle C_{J_z, J_{z'} - 1} + \langle J_x | J_x + 1 \rangle C_{J_z, J_{z'} + 1} = J_z C_{J_z, J_{z'}}.$$

The angular correlation function is then given by

$$\begin{aligned} W_{\alpha, \gamma}(\theta) &= \sum_{i, j_z} \left| \sum_l (2l+1)^{\frac{1}{2}} f_r(l) \langle j, j_z; l, 0 | J_r, J_{rz} \rangle \right. \\ &\quad \times \sum_{J_{rz'}, l'} C_{J_{rz}, J_{rz'}} (2l'+1)^{\frac{1}{2}} f_s(l') \\ &\quad \times \langle J_r, J_{rz'} | J_s, J_{sz'}; l', 0 \rangle \mathbf{E}_{J_s^{J_{sz'}}}(\theta, \varphi) \left. \right|^2. \end{aligned}$$

Here  $\theta$  represents the angle between alpha-particle and gamma-ray, and  $\varphi$ , the angle between the  $p$ - $\alpha$  plane and the  $\alpha$ - $\gamma$  plane. An equivalent treatment is to transform to the  $z'$  axis before considering formation of the compound  $Ne^{20}$ . (We are grateful to Mr. G. A. Jones for suggesting this method.) In this case an incident proton wave described by  $P_l(\cos\theta)$  can be expressed as a coherent superposition of the  $(2l+1)$  spherical harmonics  $Y_{l', m'}(\theta', \varphi')$ , where angles  $\theta$  are measured relative to  $z$  and  $(\theta', \varphi')$  relative to  $z'$ . The transformation coefficients are the spherical harmonics  $Y_{l', m'}(\theta_\alpha, 0)$  (see, for example, Smythe<sup>13</sup>). By this method the  $(\alpha, \gamma)$  correlation in a plane perpendicular to the proton beam is given by

$$\begin{aligned} W_{\alpha, \gamma}(\theta) &= \sum_{i, j_z} \left| \sum_{l, m'} f_r(l) Y_{l, m'}(\pi/2, 0) \right. \\ &\quad \times \langle j, j_z; l, m' | J_r, J_{rz} \rangle \sum_{l'} (2l'+1)^{\frac{1}{2}} f_s(l') \\ &\quad \times \langle J_r, J_{rz'} | J_s, J_{sz'}; l', 0 \rangle \mathbf{E}_{J_s^{J_{sz'}}}(\theta, \varphi) \left. \right|^2. \end{aligned}$$

### (e) Tabulation of the Formulas

In Table I we have set out the explicit formulas for  $(p, \alpha)$ ,  $(p, \gamma)$ , and  $(\alpha, \gamma)$  correlations for those quantum states of  $Ne^{20}$  and  $O^{16}$  that are of possible relevance to our experiments. Where two angular momenta of protons or alpha-particles contribute to the reaction, we put

$$f_r(l+2)/f_r(l) = A e^{i\alpha}, \quad f_s(l'+2)/f_s(l') = B e^{i\beta}.$$

Thus,  $\alpha$  and  $\beta$  represent the phase differences between

<sup>12</sup> L. I. Schiff, *Quantum Mechanics* (McGraw-Hill Book Company, Inc., New York, 1949), p. 143.

<sup>13</sup> W. R. Smythe, *Static and Dynamic Electricity* (McGraw-Hill Book Company, Inc., New York, 1949), p. 151.

TABLE I. Theoretical angular correlation patterns. [Note: In transitions from (2,-) levels of Ne<sup>20</sup> the (α,γ) pattern depends on the angle φ (Sec. III(d)) since l≠0. The formulas given are obtained for φ=90°.]

<sup>20</sup> Ne		<sup>16</sup> O	(1,-)	(1,+)	(2,-)
λ=0,2	(1,+)		l' = 1	l' = 0,2	l' = 1,3
		(p,α)	$\frac{1}{\sqrt{2}} A \cos \alpha (-1 + 3x)$ $+\frac{8}{16} A^2 (41 - 39x)$	$1 + B^2$ $+\sqrt{2} A \cos \alpha (\sqrt{2} B \cos \beta - \frac{1}{2} B^2) (-1 + 3x)$ $+\frac{1}{20} A^2 [14 - 13\sqrt{2} B \cos \beta (-1 + 3x) + \frac{3}{2} B^2 (5 + 13x)]$	$1 + B^2$ $+\frac{1}{5\sqrt{2}} A \cos \alpha (1 + 2\sqrt{2} B \cos \beta + 4 B^2) (1 - 3x)$ $+\frac{1}{200} A^2 [(127 + 39x) + 78\sqrt{6} B \cos \beta (-1 - 3x) + 4 B^2 (12 + 39x)]$
		(p,γ)	$\frac{1}{2\sqrt{2}} A \cos \alpha (1 - 3x)$ $+\frac{8}{16} A^2 (43 + 39x)$	$1 + B^2$ $+\frac{1}{\sqrt{2}} A \cos \alpha (1 + \frac{1}{10} B^2) (-1 + 3x)$ $+\frac{1}{40} A^2 [(41 - 39x) + \frac{1}{10} B^2 (293 - 39x)]$	$1 + B^2$ $+\frac{1}{2\sqrt{2}} A \cos \alpha (1 + \frac{3}{10} B^2) (1 - 3x)$ $+\frac{1}{80} A^2 [(43 + 37x) + \frac{3}{10} B^2 (61 + 13x)]$
(α,γ)	$1 + x$	$1$ $+\frac{1}{\sqrt{2}} B \cos \beta (-1 + 3x)$ $+\frac{1}{4} B^2 (5 - 3x)$	$1 + x$ $+ 2\sqrt{3} B \cos \beta (1 - 9x + 10x^2)$ $+\frac{3}{2} B^2 (1 + 6x - 5x^2)$		
λ=1,3	(2,-)		l' = 2	l' = 1,3	l' = 0,2,(4)
		(p,α)	$1 + x$ $+ 2\sqrt{\frac{2}{3}} A \cos \alpha (1 - 9x + 10x^2)$ $+\frac{2}{3} A^2 (1 + 6x - 5x^2)$	$(1 + \frac{2}{3}x) + \frac{2\sqrt{6}}{3} B \cos \beta (1 - 3x) + \frac{13}{15} B^2 (1 + 2x)$ $+\frac{1}{15} \sqrt{\frac{2}{3}} A \cos \alpha [(1 - 3x) + 2\sqrt{6} B \cos \beta (-21x + 25x^2) + B^2 (1 + 18x - 25x^2)]$ $+\frac{1}{15} A^2 [(1 + 2x) + \frac{1}{15} B \cos \beta (-1 + 18x - 25x^2) + \frac{1}{15} B^2 (3 + 6x + 25x^2)]$	$1 + \sqrt{\frac{6}{5}} B \cos \beta (1 - 3x) + \frac{13}{30} B^2 (31 - 9x)$ $+\sqrt{6} A \cos \alpha [\frac{\sqrt{6}}{15} B \cos \beta (-1 + 3x) + \frac{1}{15} B^2 (-1 + 9x - 10x^2)]$ $+ A^2 [1 + 4\sqrt{\frac{6}{35}} B \cos \beta (1 - 3x) + \frac{1}{15} B^2 (7 - 18x + 15x^2)]$
		(p,γ)	$1 + \frac{7}{11}x$ $+\frac{2}{11} \sqrt{\frac{2}{3}} A \cos \alpha (1 - 3x)$ $+\frac{8}{33} A^2 (4 + 3x)$	$(1 - \frac{2}{11}x) + \frac{1}{11} B^2 (7 - x)$ $+\frac{1}{11} \sqrt{\frac{2}{3}} A \cos \alpha (1 + \frac{1}{11} B^2) (-1 + 3x)$ $+\frac{2}{11} A^2 [(2 - x) + \frac{1}{11} B^2 (37 - 6x)]$	$(1 + x) + \frac{1}{2} B^2 (59 - 9x)$ $+ 2\sqrt{\frac{2}{3}} A \cos \alpha [(1 - 9x + 10x^2) + \frac{1}{15} B^2 (3 - 33x + 40x^2)]$ $+\frac{2}{3} A^2 [(1 + 6x - 5x^2) + \frac{1}{3} B^2 (7 + 3x - 5x^2)]$
(α,γ)	$x$	$1 - \frac{4}{13}x$ $+\frac{6}{13} \sqrt{\frac{2}{3}} B \cos \beta (1 + 2x)$ $+\frac{13}{13} B^2 (1 - \frac{1}{2}x)$	$\frac{1}{14} B \cos \beta (2 - 3x)$ $+\frac{5}{14} B^2 (4 + 13x - 16x^2)$		

<sup>20</sup> Ne		<sup>16</sup> O	(2,+)	(3,-)	(3,+)
λ=0,2	(1,+)		l' = 2	l' = 3	l' = 2,4
		(p,α)	$\frac{1}{\sqrt{2}} A \cos \alpha (-1 + 3x)$ $+\frac{8}{20} A^2 (41 - 39x)$	$1$ $+\frac{1}{\sqrt{2}} A \cos \alpha (-1 + 3x)$ $+\frac{1}{40} A^2 (41 - 39x)$	$1 + B^2$ $+\frac{1}{4\sqrt{2}} A \cos \alpha (1 - 6\sqrt{3} B \cos \beta + \frac{5}{2} B^2) (1 - 3x)$ $+\frac{1}{140} A^2 [(85 + 39x) + 78\sqrt{3} B \cos \beta (-1 - 3x) + \frac{1}{2} B^2 (31 + 195x)]$
		(p,γ)	$\frac{1}{2\sqrt{2}} A \cos \alpha (-1 + 3x)$ $+\frac{8}{80} A^2 (23 - 13x)$	$1$ $+\frac{3}{4\sqrt{2}} A \cos \alpha (-1 + 3x)$ $+\frac{1}{160} A^2 (151 - 117x)$	$1 + B^2$ $+\frac{3}{24\sqrt{2}} A \cos \alpha (1 + \frac{3}{15} B^2) (1 - 3x)$ $+\frac{1}{200} A^2 [(101 + 117x) + \frac{15}{2} B^2 (33 + 13x)]$
(α,γ)	$1 - 3x + 4x^2$	$1 + 111x - 305x^2 + 225x^3$	$1 + \frac{6}{10}x + x^2$ $+\frac{1}{10} \sqrt{3} B \cos \beta (-11 + 243x - 725x^2 + 525x^3)$ $+\frac{3}{40} B^2 (17 - 65x + 255x^2 - 175x^3)$		
λ=1,3	(2,-)		l' = 1,3	l' = 2,4	l' = 1,3,(5)
		(p,α)	$(1 - \frac{7}{3}x) + \frac{4}{3} B \cos \beta (1 - 3x) + \frac{2}{3} B^2 (3 + x)$ $+\frac{2}{3} \sqrt{\frac{2}{3}} A \cos \alpha [(1 + 3x) + 2B \cos \beta (-3 + 24x - 25x^2) + \frac{1}{2} B^2 (7 - 66x + 75x^2)]$ $+\frac{2}{27} A^2 [(7 - 6x) + \frac{1}{2} B \cos \beta (9 - 42x + 25x^2) + \frac{1}{27} B^2 (29 + 78x - 75x^2)]$	$(1 - \frac{2}{3}x) + \frac{1}{3} \sqrt{\frac{2}{3}} B \cos \beta (1 - 3x) + \frac{1}{3} B^2 (9 + x)$ $+\frac{1}{18} A \cos \alpha [(-1 - 6x + 15x^2) + 4\sqrt{2} B \cos \beta (-3 + 24x - 25x^2) + 2B^2 (4 - 39x + 45x^2)]$ $+\frac{1}{12} A^2 [(73 - 42x - 15x^2) + 4\sqrt{2} B \cos \beta (9 - 42x + 25x^2) + 2B^2 (23 + 42x - 45x^2)]$	$(1 + \frac{1}{3}x) + \frac{4}{30} B \cos \beta (1 - 3x) + \frac{1}{30} B^2 (71 - 33x)$ $+\frac{2}{31} \sqrt{\frac{2}{3}} A \cos \alpha [(1 - 3x) + \sqrt{3} B \cos \beta (-3 - 6x + 25x^2) + \frac{1}{2} B^2 (-8 + 69x - 75x^2)]$ $+\frac{2}{93} A^2 [(31 + 12x) + \frac{1}{2} \sqrt{3} B \cos \beta (39 - 102x - 25x^2) + \frac{1}{93} B^2 (79 - 102x + 75x^2)]$
		(p,γ)	$(1 + \frac{2}{3}x) + \frac{8}{9} B^2 (8 - 3x)$ $+\frac{2}{3} \sqrt{\frac{2}{3}} A \cos \alpha [(-3 + 33x - 40x^2) + \frac{1}{2} B^2 (-1 + 6x - 5x^2)]$ $+\frac{8}{21} A^2 [(3 - 3x + 5x^2) + \frac{1}{21} B^2 (33 - 18x + 5x^2)]$	$(1 + \frac{2}{3}x) + \frac{8}{9} B^2 (19 - 9x)$ $+\frac{2}{3} \sqrt{\frac{2}{3}} A \cos \alpha [(3 - 24x + 25x^2) + \frac{1}{2} B^2 (-3 + 3x + 10x^2)]$ $+\frac{1}{4} A^2 [(71 + 42x - 25x^2) + \frac{1}{4} B^2 (87 - 42x - 5x^2)]$	$(1 + \frac{2}{3}x) + \frac{1}{50} B^2 (91 - 33x)$ $+\frac{1}{70} A \cos \alpha [(3 + 6x - 25x^2) + \frac{1}{2} B^2 (-9 + 57x - 50x^2)]$ $+\frac{1}{94} A^2 [(81 + 102x + 25x^2) + B^2 (141 - 78x + 25x^2)]$
(α,γ)	$1 - \frac{4}{3}x$ $+\frac{2}{3} B \cos \beta (4x - 5x^2)$ $+\frac{1}{3} B^2 (5 - 16x + 15x^2)$	$1 + \frac{2}{3}x - \frac{1}{3}x^2$ $+\frac{1}{3} \sqrt{\frac{2}{3}} B \cos \beta (10 - 151x + 440x^2 - 315x^3)$ $+\frac{1}{10} B^2 (4 + 109x - 286x^2 + 189x^3)$	$1 + 7x$ $+\frac{1}{4} \sqrt{3} B \cos \beta (13 + 46x - 75x^2)$ $+\frac{7}{96} B^2 (197 - 1206x + 3525x^2 - 2500x^3)$		

interfering states of the system,  $A$  and  $B$  their relative amplitudes. One simplification has been made in setting up the table, namely, the restriction of  $l$  (but not  $l'$ ) to its lowest value only in the formulas for  $(\alpha, \gamma)$  correlations. This has some justification (see Sec. VI below). All angular distributions are expressed for brevity in powers of  $x = \cos^2\theta$ ; the absence of odd powers of  $\cos\theta$  comes from our initial assumption that there is no interference between different states in  $Ne^{20}$  and  $O^{16}$ .

#### (f) Evaluation of Phase Shifts

According to the modern dispersion theory (Wigner and Eisenbud<sup>14</sup>) the intrinsic widths of nuclear levels are real, so that the phase shifts  $\alpha$  and  $\beta$  (apart from an uncertainty of  $\pi$ ) are due entirely to the Coulomb and angular momentum barriers. In our problem there is no relative phase shift associated with the resonance denominator ( $E - E_r + \frac{1}{2}i\Gamma_r$ ) since it remains the same for all orbital momenta, only one nuclear level in  $Ne^{20}$  or  $O^{16}$  being involved.

The phase shift associated with an orbital momentum  $l$  in a Coulomb field is given (e.g., Bloch *et al.*<sup>15</sup>) by

$$\delta_l = -\tan^{-1}(F_l/G_l) - \eta \log(2kR) + \sigma_l - \frac{1}{2}l\pi,$$

where the quantities have their usual significance, *viz.*,  $F_l$ ,  $G_l$  are the regular and irregular solutions of the Coulomb wave equation;  $\eta = (Z_1 Z_2 e^2 / \hbar v)$ ;  $k = \mu v / \hbar$ ,  $\mu$  being the reduced mass of the system;  $R$  = nuclear radius; and  $\sigma_l = \arg\Gamma(l+1+i\eta)$ .

In the present reaction the proton and alpha-particle energies are well below the respective barrier heights, so that  $F_l \ll G_l$ , and the phase difference between two waves of orbital momenta  $l$ ,  $l+2$  becomes

$$\begin{aligned} \delta_{l, l+2} &= \sigma_{l+2} - \sigma_l - \pi \\ &= \tan^{-1} \frac{\eta}{l+2} + \tan^{-1} \frac{\eta}{l+1} - \pi. \end{aligned}$$

The numerical values of  $\cos\alpha$  and  $\cos\beta$  are therefore determined by the energies and orbital momenta of the protons and alpha-particles, and do not depend on a choice of nuclear radius. Thus, the only parameters at our disposal in fitting an observed correlation are the magnitudes of  $A$  and  $B$  and the signs of  $\cos\alpha$  and  $\cos\beta$ .

### IV. EXPERIMENTAL METHOD

#### (a) Angular Correlations

##### (1) Detectors

At the 340-keV resonance, the  $\alpha_1$ -particles have a longer range than the scattered protons, so that measurements on the  $(\alpha_1, \gamma)$  and  $(p, \alpha_1)$  correlations can be made with a proportional counter or ionization chamber with a thin window to exclude the protons. For the higher

<sup>14</sup> E. P. Wigner and L. Eisenbud, *Phys. Rev.* **72**, 29 (1947).

<sup>15</sup> Bloch, Hull, Broyles, Bouricius, Freeman, and Breit, *Revs. Modern Phys.* **23**, 147 (1951).

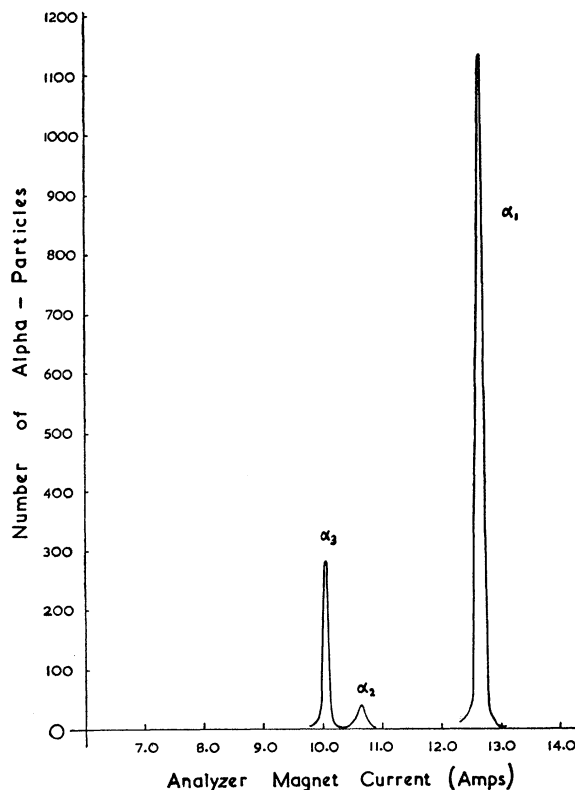


FIG. 2. Alpha-particle spectrum at 935-keV proton energy.

resonances, all three alpha-particle groups have shorter ranges than the scattered protons, and some form of energy analysis becomes necessary. The most convenient method, also allowing complete separation of the alpha-particle groups from each other, is to use a magnetic spectrometer.

In the early stages of the work an analyzer with 60° inflection focusing was used. It had a resolution of 4 percent in energy and a solid angle of 1/5000 of a sphere. In the  $(\alpha, \gamma)$  angular correlation measurements alpha-particles emitted at 90° to the incident proton beam were observed; the detector was a thin zinc sulfide screen with photomultiplier. In conjunction with this, a liquid scintillation counter was used to detect the gamma-rays. The phosphor was a 2 percent solution of terphenyl in toluene which subtended a solid angle of 1/25 of a sphere at the target, and had a counting efficiency of 10 percent for 7-MeV gamma-rays. With this arrangement it was possible to study angular correlations for the more intense alpha-particle groups.

A substantial improvement in the experiments was effected later when a 180° double focusing magnetic analyzer for the alpha-particles and a sodium iodide scintillation counter for the gamma-rays became available. The magnet was designed by Dr. J. M. Freeman and is of the type described by Snyder *et al.*<sup>16</sup> It has a

<sup>16</sup> Snyder, Rubin, Fowler, and Lauritsen, *Rev. Sci. Instr.* **21**, 852 (1950).

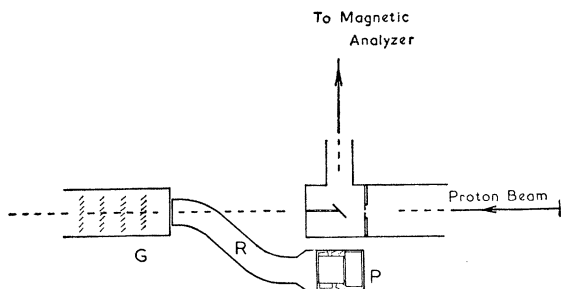


FIG. 3. Schematic diagram of experimental arrangement.

solid angle of  $1/1500$  sphere with a resolution of 4 percent in energy. Figure 2 shows a typical alpha-particle spectrum obtained with this analyzer and serves to demonstrate the complete separation of the groups.

Figure 3 shows the general arrangement. The alpha- and gamma-detectors were placed so as to measure the angular correlation in the plane perpendicular to the proton beam. The gamma-photomultiplier  $G$  was mounted along the axis of the proton beam, and was not moved during the measurements. The phosphor  $P$  could be rotated about this axis and the scintillations were conveyed to the photomultiplier by a curved Perspex rod  $R$  of  $1''$  diameter enclosed in a light-tight brass case. This construction was adopted to avoid changes of gain of the photomultiplier which would result from moving it in the stray magnetic field. The angular aperture of the gamma-phosphor was about  $35^\circ$ ; this was obtained in the later arrangement with a  $1\frac{1}{2}$  in.  $\times$   $1\frac{1}{2}$  in. mosaic of sodium iodide crystals placed  $2\frac{1}{4}$  in. from the target. The large angle of the gamma-detector, together with an intrinsic detection efficiency of 35 percent, helped to compensate for the small solid angle of the alpha-particle detector.

Although the main use of the improved apparatus was to study the weaker reactions, the work on the more intense reactions was repeated for the sake of completeness, and all angular correlations illustrated in this paper were obtained with the new system.

### (2) Coincidence Circuits

The outputs of the alpha- and gamma-photomultipliers were amplified and fed into a coincidence circuit of conventional design having a resolving time of  $0.3 \mu\text{sec}$ . The amplified pulses from the gamma-detector were delayed by about  $0.15 \mu\text{sec}$  before being put into coincidence, in order to compensate for the time of flight of the alpha-particles in the spectrometer. As the fraction of random coincidences in the total coincidence count was appreciable, the random coincidence counting rate was continuously monitored: The alpha-particle pulses were delayed by  $2 \mu\text{sec}$  and put into coincidence with the gamma-ray pulses in a second and identical

coincidence unit. (This method is described by Littauer.<sup>17</sup>)

### (3) Experimental Procedure

In all the experiments the target was a thin  $\text{CaF}_2$  layer (5 keV for 500-keV protons) evaporated on a copper foil 0.004 inch thick. The proton beam current was continuously monitored and was maintained at about 1 to  $2 \mu\text{A}$  so as to secure a real to random coincidence ratio of at least unity. Besides the real and random coincidence rates, the individual alpha- and gamma-counts were measured. After a desired alpha-particle group had been selected with the magnetic analyzer, alpha-gamma coincidences were measured for 15-minute periods at a series of angles between  $90^\circ$  and  $180^\circ$ . An average of six measurements was made for each angle, and observations were made at  $15^\circ$  intervals in most of the correlations.

The alpha-particle counting rate with the later arrangement varied from about 100 per minute ( $\alpha_2$  at 935 keV) to 3000 per minute ( $\alpha_1$  at all resonances). The corresponding real coincidence rate was between 1 and 50 per minute. It is perhaps of some interest to note that in the most favorable cases a correlation could be established to a few percent in  $1\frac{1}{2}$  hours. At the other extreme the ( $\alpha_2, \gamma$ ) correlation at 935 keV took 25 hours, the  $\alpha_2$  group having an intensity of only 3 percent of the main group (see Fig. 2).

### (b) Angular Distributions

Measurements were made at the 874-keV resonance on the angular distributions of the alpha-particle groups. This work was done with the  $60^\circ$  magnetic analyzer at three angles only ( $90^\circ$ ,  $120^\circ$ ,  $135^\circ$ ). The arrangement was far from ideal, but the results were of value in establishing the level schemes.

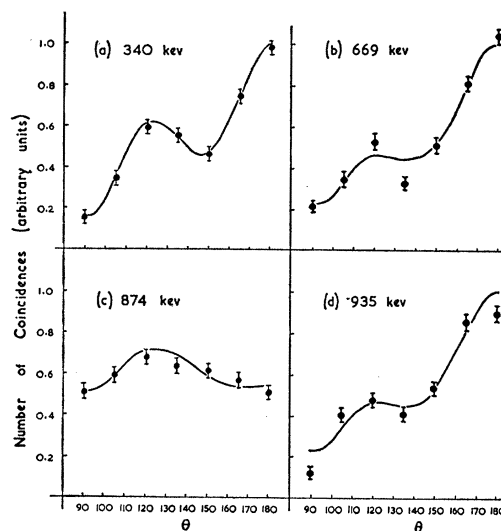


FIG. 4. ( $\alpha_1, \gamma$ ) correlations.

<sup>17</sup> R. M. Littauer, Rev. Sci. Instr. 21, 750 (1950).

## V. RESULTS

 (a)  $(\alpha_1, \gamma)$  Correlations

Figure 4 shows our results for the  $(\alpha_1, \gamma)$  correlations at the 669-, 874-, and 935-keV proton resonances in  $Ne^{20}$ . The 340-keV curve, from Barnes *et al.*,<sup>5</sup> is inserted for comparison. The full curves in (a), (b), and (d) represent the modification by the finite geometry of the apparatus of a pure octupole pattern:

$$I(\theta) = 1 + 111 \cos^2\theta - 305 \cos^4\theta + 225 \cos^6\theta.$$

It can be seen that in each case the curve is a good fit to the experimental points. Following the analysis given by Barnes *et al.*,<sup>5</sup> we can infer with certainty that the  $Ne^{20}$  resonance levels at 669- and 935-keV proton energy have spin 1 and even parity. This was suspected previously (Chao<sup>6</sup>) because of the isotropy of the gamma-rays relative to the protons at these resonances (Devons and Hine,<sup>10</sup> Day *et al.*<sup>18</sup>). More recent work by Sanders<sup>19</sup> on the angular distributions of the gamma-rays has shown that they are separately isotropic at 935 keV, so that it is probable that this level is formed mainly by  $s$  protons.

From curve (c) of Fig. 4 it is apparent that the 874 keV level is not  $(1, +)$ . Possible alternatives are  $(2, -)$  and  $(3, +)$ , and the latter is unlikely since the  $(\alpha_1, \gamma)$  correlation due to it would be very strongly anisotropic. Assuming that the level is  $(2, -)$  and is formed by  $p$  protons, the theoretical correlation in a plane at an angle  $\varphi$  to the proton beam is given by

$$\begin{aligned} I(\theta, \varphi) \sim & (25 + 46 \cos^2\theta - 55 \cos^4\theta) \\ & + \cos^2\varphi(1 - 131 \cos^2\theta + 355 \cos^4\theta - 225 \cos^6\theta) \\ & + (\sqrt{10})B \cos\beta[(10 - 151 \cos^2\theta + 440 \cos^4\theta - 315 \cos^6\theta) \\ & + \cos^2\varphi(-1 + 131 \cos^2\theta - 355 \cos^4\theta + 225 \cos^6\theta)] \\ & + (5/2)B^2[(4 + 109 \cos^2\theta - 286 \cos^4\theta + 189 \cos^6\theta) \\ & + \cos^2\varphi(1 - 131 \cos^2\theta + 355 \cos^4\theta - 225 \cos^6\theta)]. \end{aligned}$$

$B$  and  $\beta$  give the relative amplitude and phase of alpha-particles having  $l'=4$  and 2, respectively. The full curve in the figure is calculated for  $A=0$ ,  $B=0.54$ ,  $\cos\beta=-0.245$ , and is corrected for the spread in  $\theta$  and  $\varphi$  due to the finite geometry of the apparatus, the average value of  $\varphi$  being  $\pi/2$ . The size of  $\cos\beta$  is obtained theoretically [Sec. III(f)], and its sign and the value of  $B$  are chosen to give the best fit to the experimental points.

We consider that these assignments for the  $Ne^{20}$  levels [ $(1, +)$  at 669 keV,  $(2, -)$  at 874 keV,  $(1, +)$  at 935 keV] are almost certainly correct, and we shall now use them in discussing the transitions to the third and fourth excited levels in  $O^{16}$ .

 (b)  $(\alpha_2, \gamma)$  Correlations

Figure 5 shows the  $(\alpha_2, \gamma)$  correlations obtained at the 874- and 935-keV resonances in  $Ne^{20}$ . (The correla-

<sup>18</sup> Day, Chao, Fowler, and Perry, Phys. Rev. 80, 131 (1950).

<sup>19</sup> J. E. Sanders, Phil. Mag. 43, 630 (1952).

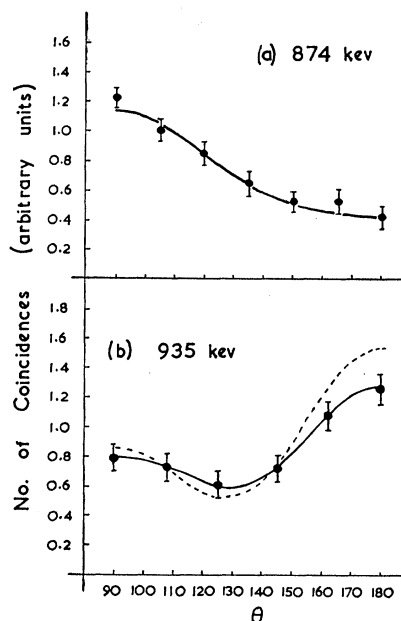


FIG. 5.  $(\alpha_2, \gamma)$  correlations.

tion at 669 keV could not be attempted because of its very low intensity.) The broken curve of Fig. 5(b) is the expected pattern (allowing for finite geometry) for a pure quadrupole correlation given by

$$I(\theta) = 1 - 3 \cos^2\theta + 4 \cos^4\theta.$$

Despite the rather poor statistics, one can see that the curve is a reasonable fit to the experimental points. This pattern can only arise if the  $\alpha_2$  particle is emitted with 2 units of orbital momentum and is followed by an electric quadrupole gamma-ray. The  $\alpha_2$  level in  $O^{16}$  would therefore be  $(2, +)$ .

Strong supporting evidence for this assignment is provided by the  $(\alpha_2, \gamma)$  correlation at 874 keV [Fig. 5(a)]. If our level assignments are correct, Table I indicates that the pattern will be dominated by a term,

$$I(\theta, \pi/2) = 1 - \frac{4}{3} \cos^2\theta,$$

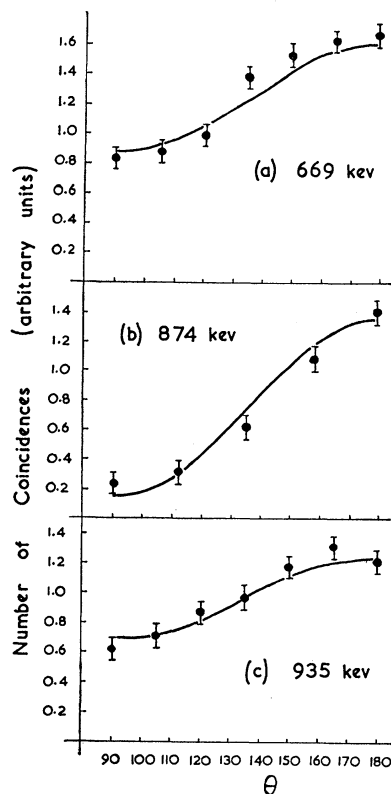
due to  $p$ -wave alpha-particles, and that the presence of  $f$ -wave alpha-particles will reduce the anisotropy. The full curve of Fig. 5(a) is obtained by putting  $A=0$ ,  $B=0.35$ ,  $\cos\beta=-0.244$ , and correcting for the finite geometry as for the  $(\alpha_1, \gamma)$  correlations. The phase angle  $\beta$  is again obtained from the Coulomb wave functions. Further support for these values comes from the  $(p, \alpha_2)$  angular distribution at 874 keV [see Sec. V(d) below].

 (c)  $(\alpha_3, \gamma)$  Correlations

Figure 6 shows the  $(\alpha_3, \gamma)$  correlations at 669, 874, and 935 keV. The curves at 669 and 935 keV can be well fitted by the formula

$$I(\theta) = 1 + \cos^2\theta.$$

This suggests that the  $\alpha_3$  level is  $(1, -)$ , although the

FIG. 6.  $(\alpha_3, \gamma)$  correlations.

pattern could also be obtained with a  $(2, -)$  level in  $O^{16}$  if  $B$  were small (see Table I). The  $(\alpha_3, \gamma)$  correlation observed at 874 keV, however, confirms the former assignment, for which the theoretical pattern is

$$I(\theta, \varphi) = \cos^2\theta \sin^2\varphi + \cos^2\varphi.$$

A satisfactory fit to the 874-keV correlation could not be obtained by assuming the  $\alpha_3$  level to be  $(2, -)$ , even with an arbitrary choice of  $\alpha$  and  $\beta$  and the introduction of terms due to alpha-particles having  $l' = 4$ .\*

All three curves of Fig. 6 are obtained by correcting the theoretical curves for the finite geometry of the apparatus, assuming  $A = 0$ .

#### (d) $(p, \alpha)$ Angular Distributions

The alpha-particle angular distributions at the 874-keV resonance are given in Fig. 7. The full curves are those calculated assuming that the 874-keV level in  $Ne^{20}$  is  $(2, -)$  and that the  $\alpha_1$ ,  $\alpha_2$ , and  $\alpha_3$  levels in  $O^{16}$  are  $(3, -)$ ,  $(2, +)$ , and  $(1, -)$ , respectively, with the values of  $B$  and  $\cos\beta$  deduced from the  $(\alpha, \gamma)$  correlations. The  $(p, \alpha_3)$  curve has special interest because the shape of the distribution is very sensitive to the value of  $A$ . Taking  $|\cos\alpha| = 0.439$  as given by the Coulomb

\* (Note added in proof: We have since measured the  $(\alpha_3, \gamma)$  correlation in the plane  $\varphi = 0$  at 874 keV. The result was isotropic within  $\pm 10$  percent, thus supporting the  $(1, -)$  assignment.)

functions, we find the value of  $A$  to be  $0.1 \pm 0.1$ . This is our justification for setting  $A = 0$  throughout our calculations. It would clearly be desirable to measure these angular distributions in more detail.

#### (e) $(p, \gamma)$ Angular Distributions

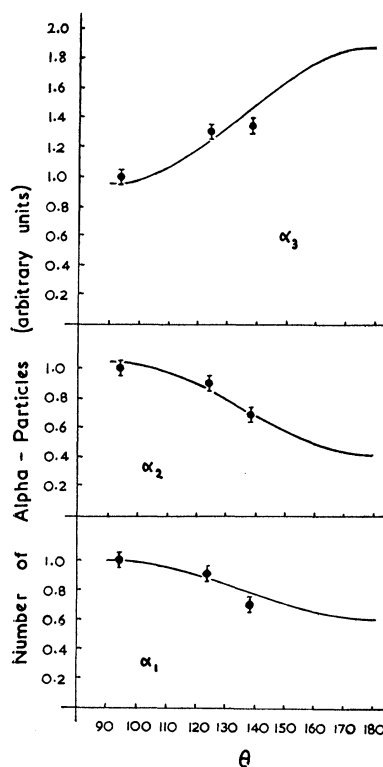
Sanders<sup>19</sup> has used a deuterium chamber to separate the 6.1-Mev gamma-rays ( $\gamma_1$ ) from the mixture ( $\gamma_2 + \gamma_3$ ) and has measured the angular distributions of these two groups at 874 and 935 keV. As we have mentioned previously, the 935-keV  $\gamma$ -rays appear to be separately isotropic. At 874 keV, Sanders found the  $(p, \gamma_1)$  distribution to be again isotropic within 5 percent, and using our values of  $A$ ,  $B$ , and  $\cos\beta$ , the expected angular distribution is

$$I_1(\theta) = 1 + 0.04 \cos^2\theta,$$

which agrees well with his results.

To compute the theoretical angular distribution for  $(\gamma_2 + \gamma_3)$  at 874 keV, we have taken the relevant parameters from our fitting of the  $(\alpha, \gamma)$  correlations, and have assumed that the over-all intensities of  $\gamma_2$  and  $\gamma_3$  are in the ratio 3:1. This approximate figure is obtained from our measurements of alpha-particle yield, taking account of the angular distributions, and the computed  $(\gamma_2 + \gamma_3)$  curve is

$$I_{2+3}(\theta) = 1 + 0.36 \cos^2\theta,$$

FIG. 7.  $(p, \alpha)$  distributions.

whereas Sanders found

$$I_{2+3}(\theta) = 1 + 0.32 \cos^2\theta,$$

which agrees within the errors of the observations.

## VI. DISCUSSION

The results described above have suggested a complete level scheme for the reactions  $F^{19}(p, \alpha\gamma)$ . It is illustrated in Fig. 8. The theoretical analysis has been given very briefly so as not to obscure the main arguments, and it may seem at first sight that several other level schemes could fit the experiments. When the detailed comparison with Table I is carried out, however, one finds that the choice of levels is very limited.

The identification of the states taking part in a given transition has been made in the first instance from the  $(\alpha, \gamma)$  angular correlation pattern. One can see from Table I that when a mixture of two orbital momenta for the alpha-particles is possible the shape of the pattern may be strongly modified. Despite this complication, any one correlation measurement usually gives the parity of a given level in  $O^{16}$  without any ambiguity, and limits the choice of angular momentum ( $J$ ) to two or, at most, three values. The combined evidence from our total of nine angular correlation measurements then leads to a unique value of  $J$  for each level in  $O^{16}$ . The experiments are not accurate enough to establish the precise values of the amplitude and phase factors ( $A, \alpha$ ) and ( $B, \beta$ ), but at 874 keV, where we have evidence for the  $(p, \alpha)$  and  $(p, \gamma)$  correlations as well as the  $(\alpha, \gamma)$ , the same set of values of  $B$ , together with the theoretical phase shifts, will fit all three measurements for a given level in  $O^{16}$ .

We have mentioned earlier (Sec. III) that we have not considered more than one orbital momentum for the incoming protons in obtaining the theoretical expressions of Table I for  $(\alpha, \gamma)$  correlations. This is on the whole justifiable for a correlation observed in a plane at right angles to the proton beam, as the essential features of the pattern are not affected by a contribution from higher  $l$  values. (We have checked this in individual cases.) No such simplification can be made for correlations observed in a plane containing the proton beam direction, nor, of course, for the angular distributions of alpha-particles and gamma-rays relative to the protons. One drawback of our simplified scheme is that the quantities ( $B, \beta$ ) must now serve to describe the mixing both of incoming proton waves and of outgoing alpha-particle waves. Their physical significance is thus slight unless the reaction is dominated by the lowest possible orbital momentum for the protons, which does seem to be the case in the present reaction.

Certain features of the results may be specially noted. So far as one can tell, there is no difference in properties of the 669- and 935-keV resonance levels in  $Ne^{20}$ . Both the  $(\alpha_1, \gamma)$  and the  $(\alpha_3, \gamma)$  correlations are identical within the accuracy of the measurements. The occurrence of radiative capture at 669-keV proton energy

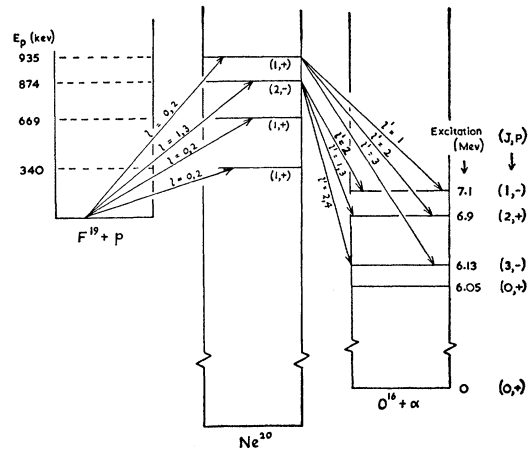


FIG. 8. Level scheme for the reaction  $F^{19}(p, \alpha\gamma)O^{16}$ .

and not at 340 or 935 keV (Devons and Hereward<sup>20</sup>) is therefore rather surprising, if indeed the capture gamma-ray comes from the same state as the alpha-particles. A careful study by J. E. Sanders (private communication) has failed to reveal any difference between the excitation functions for the two processes.

The difficulty of drawing reliable conclusions from considerations of potential barrier penetrability is well known. In the present reaction it is interesting to compare the observed branching ratio between the alpha-particles with what one would expect for the orbital momenta involved. To make the comparison we have computed the penetrabilities by simple barrier theory (WKB method as presented by Bethe<sup>21</sup>) for the orbital momenta suggested by our analysis, and have normalized them so that the sum of all three alpha-particle intensities at a given resonance is unity. The experimental branching ratios are taken from the results of Freeman,<sup>22</sup> corrected for angular distribution according to Fig. 7 of the present paper and normalized in the same way. The results are given in Table II. It may be seen that there is a rough correspondence between theory and experiment except for the  $\alpha_3$  group at 874 keV and the  $\alpha_2$  group at 669 and 935 keV. These last modes of decay seem to be strongly discouraged.

TABLE II. Branching of competing alpha-particle emissions. The upper figure of each pair is the computed branching ratio.

	$\alpha_1$	$\alpha_2$	$\alpha_3$
669 keV	0.68	0.13	0.19
	0.82	0.003	0.17
874 keV	0.82	0.17	0.01
	0.74	0.19	0.07
935 keV	0.49	0.18	0.33
	0.75	0.03	0.22

<sup>20</sup> S. Devons and H. G. Hereward, *Nature* **162**, 331 (1948).

<sup>21</sup> H. A. Bethe, *Revs. Modern Phys.* **9**, 177 (1937).

<sup>22</sup> J. M. Freeman, *Phil. Mag.* **41**, 1225 (1950).

It is perhaps worth remarking on the successful application of modern dispersion theory to predict phase differences between interfering states. The present reaction is especially amenable to a comparison with the theory because the levels are narrow and clearly separated, and the particle energies are well below the barrier heights.

#### VII. THE ALPHA-PARTICLE MODEL OF $O^{16}$

The development of the alpha-particle model by Wheeler<sup>23</sup> and Dennison<sup>3</sup> was carried out when little was known of the spins and parities of individual nuclear states. The link between theory and experiment was provided essentially by some rather indefinite evidence on the resonant scattering of alpha-particles in helium (Wheeler<sup>23</sup>) and by the discovery of the pair-emitting state of  $O^{16}$  (Fowler and Lauritsen<sup>24</sup>). This, together with a knowledge of the binding energy of one alpha-particle in the nuclei  $C^{12}$  and  $O^{16}$  in their ground states, made it possible to advance plausible values for the rotational and vibrational energies of an alpha-particle system. The symmetry of the system then imposed limitations on the quantum numbers of the excited states, and tentative level schemes could be set up.

The picture of  $O^{16}$  as a regular tetrahedron implies that it has characteristic frequencies for pulsation, twisting, and flattening; these are usually denoted by  $\omega_1$ ,  $\omega_2$ , and  $\omega_3$ , respectively, and are in the ratio of approximately  $2:1:\sqrt{2}$ . The lowest nonrotational state allowed by the symmetry is a pulsating mode with energy  $\hbar\omega_1$ , zero total angular momentum, and even parity. It thus reproduces the properties of the pair state very well. On the other hand, one would expect the lowest rotational state, with no vibration, to lie at a lower energy than the pair level at 6.05 Mev. Symmetry requires that it should have the designation  $(3,-)$ , and a conventional figure ( $\sim 4 \times 10^{-13}$  cm) for the nuclear radius, on which the energy alone depends, would place such a level at about 2 Mev.

Since there is almost certainly no excited state of nonzero spin below 6.05-Mev excitation in  $O^{16}$ , it seems reasonable to identify the 6.13-Mev level with this pure rotational state, and to make use of this identification to deduce an effective moment of inertia for the oxygen nucleus. The corresponding nuclear radius is  $2.5 \times 10^{-13}$  cm. This is less than the accepted value by about the range of nuclear forces, and might

perhaps represent the mean distance of nuclear particles from the center of the nucleus.

If we take the first two states in  $O^{16}$  as defining the parameters for the higher rotational-vibrational levels, we find that the next three levels would be a doublet  $(2,+; 2,-)$  and a singlet  $(1,-)$  in ascending order. The splitting of the doublet is due to an inversion mechanism, and its size cannot be accurately predicted, although according to Dennison<sup>3</sup> it should be small. It is satisfactory that the  $(2,+)$  and  $(1,-)$  levels do occur in the predicted order, but the absence of the  $(2,-)$  level remains an anomaly.

The treatment given by Dennison<sup>3</sup> does not assume that  $\omega_1$  is exactly twice  $\omega_2$ . One might therefore use the following relations to establish the energies of the various modes in  $O^{16}$ :

$$\begin{aligned} \text{Pair state:} & \quad \hbar\omega_1 = 6.05 \text{ Mev,} \\ (3,-) \text{ state:} & \quad 6\hbar^2/I = 6.13 \text{ Mev,} \\ (1,-) \text{ state:} & \quad (17\hbar^2/8I) + \hbar\omega_3 = 7.11 \text{ Mev.} \end{aligned}$$

With these assumptions it is possible to estimate the approximate level density for higher excitations of an alpha-particle structure. In the region 12- to 13.5-Mev excitation the predicted level spacing in  $O^{16}$  agrees fairly well with that found by Schardt *et al.*<sup>25</sup> in a study of the  $N^{15}(p,\alpha\gamma)$ ,  $N^{15}(p,\alpha)$ , and  $N^{15}(p,\gamma)$  reactions. Other regions of excitation have not been studied in sufficient detail to make an extensive comparison possible.

#### VIII. CONCLUDING REMARKS

This study of the  $F^{19}(p,\alpha\gamma)$  reaction seems to bear out the usefulness of the alpha-particle model as a description of the low states of  $O^{16}$ . It is certainly rather difficult to describe all first four states in terms of the shell model.

Although it is unlikely that the alpha-particle model will remain valid above the first few excited states, it would be interesting to carry the comparison of theory with experiment to higher levels in this nucleus, particularly those in the region between 8 and 12 Mev, which has not yet been thoroughly studied. One might also hope to obtain fuller information about the level structure of  $Be^8$  and  $C^{12}$ , and to find whether these related systems can be incorporated within the same theoretical framework.

One of us (J.S.) is indebted to the Department of Scientific and Industrial Research for the tenure of a research grant over the period in which this work was performed.

<sup>23</sup> J. A. Wheeler, Phys. Rev. **59**, 16 (1941).

<sup>24</sup> W. A. Fowler and C. C. Lauritsen, Phys. Rev. **56**, 840 (1939).

<sup>25</sup> Schardt, Fowler, and Lauritsen, Phys. Rev. **86**, 527 (1952).